Hindawi Publishing Corporation
International Journal of Antennas and Propagation
Volume 2008, Article ID 792123, 5 pages
doi:10.1155/2008/792123

Research Article

Analysis and Design of Gap-Coupled Annular Ring Microstrip Antenna

Binod Kumar Kanaujia[1] and Anil Kumar Singh[2]

[1] *Department of Electronics and Communication Engineering, Faculty of Engineering and Technology, M. J. P. Rohilkhand University, Bareilly 243006, India*
[2] *Department of Electronics and Instrumentation Engineering, Faculty of Engineering and Technology, M. J. P. Rohilkhand University, Bareilly 243006, India*

Correspondence should be addressed to Binod Kumar Kanaujia, bk32@rediffmail.com

Received 23 December 2007; Revised 7 March 2008; Accepted 21 July 2008

Recommended by Deb Chatterjee

Theoretical investigation conducted on gap-coupled annular ring microstrip antenna is found to exhibit frequency tunability with the gap. The various parameters of the antenna such as input impedance, VSWR, return loss, and radiation pattern have been investigated as a function of gap length and feed point. It is found that the various parameters of gap-coupled microstrip antenna depend heavily on the gap length and feed points.

1. INTRODUCTION

The annular ring microstrip antenna (ARMSA) has been studied for a long time by a number of investigators [1, 2] because of larger bandwidth as compared to the other conventional microstrip patch antennas [1]. The interest in designing of such microstrip antenna has increased because of light weight, easier to fabrication, conformability, and so forth. The inner and outer radii of the ARMSA control the mode separation.

In the present work, the authors have endeavored to design a gap-coupled concentric ARMSA on the basis of equivalent circuit model. The inner ring is a feed, and the outer ring is a parasitic element. The effect of mutual coupling is also taken into account along with variation of feed point and gap between the rings. The gap-coupled ARMSA can be used for dual band operation and especially in mobile communication. The main focus is on the effect of the gap length and feed point on the radiation pattern of the gap-coupled ARMSA.

2. THEORETICAL CONSIDERATIONS

In the concentric ARMSA, the structure having physical gap is shown in Figure 1(a). The inner ring is fed coaxially, while the outer ring is a parasitic element. Now, this can also be shown as a parallel gap-coupled radiator using planar waveguide mode for inner ring and outer ring as shown in Figure 1(b) [3]. The characteristic impedance of the two-gap-coupled concentric ARMSA radiator can be analyzed by applying the theory of coupled microstrip lines [4, 5] and coupled microstrip antenna [6].

The input impedance characteristics of the gap-coupled ARMSA can be analyzed. Figure 1(a) which shows two-gap-coupled annular ring antennas in which inner one is fed at point $(x, 0)$ by a coaxial cable $(a_1 < x < b_1)$, where a_1 and b_1 are inner and outer radii of the inner ring and outer ring, respectively. The thickness of the substrate h is small as compared to the difference between the inner and outer radii of the inner ring.

2.1. Even and odd mode capacitances

Two concentric annular ring antenna having width $W_1 = b_1 - a_1$ and $W_2 = b_2 - a_2$ of Figure 1(a) can be shown, as a gap-coupled microstrip line of Figure 1(b), by using planer waveguide model. The inner ring of annular ring antenna of Figure 1(b) is excited in TM_{12} mode. Total line capacitance is taken up as a parallel plate capacitance (C_p) and two fringing

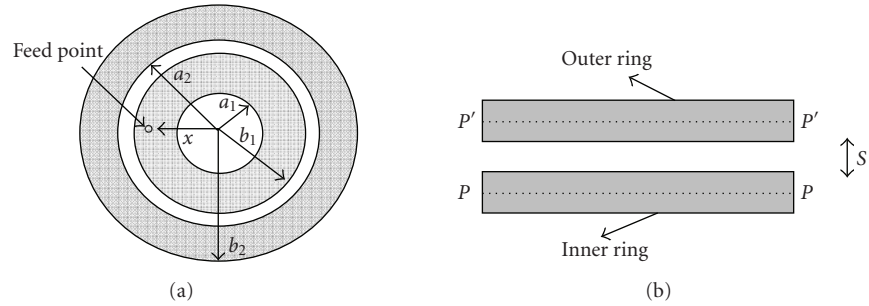

Figure 1: (a) Concentric annular ring microstrip antenna. (b) Parallel gap-coupled microstrip lines.

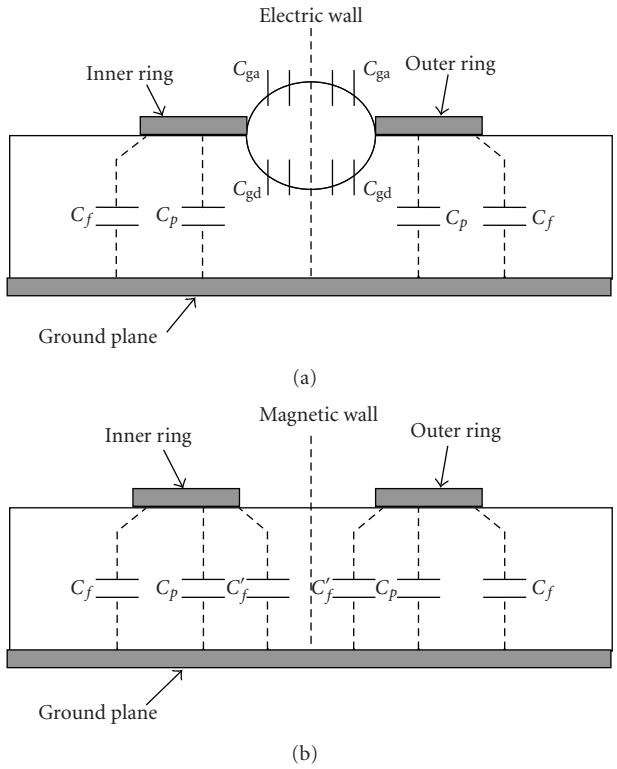

Figure 2: (a) Odd mode capacitances of coupled microstrip lines geometry. (b) Even mode capacitances of coupled microstrip lines geometry.

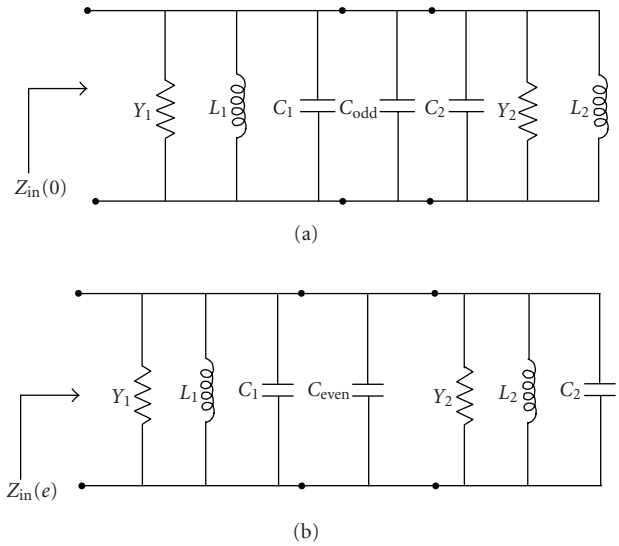

Figure 3: (a) Modified equivalent circuit of gap-coupled ARMSA for odd mode. (b) Modified equivalent circuit of gap-coupled ARMSA for even mode.

capacitances (C_f) as shown in Figures 2(a) and 2(b) for even and odd modes, respectively. The even mode capacitance is the capacitance between two parallel running conductors with respect to ground. From Figure 2(b), it is given as $C_{\text{even}} = C_p + C_f + C'_f$, where $C_p = \varepsilon_r \varepsilon_0 (w/h)$ is the parallel plate capacitance between the strip and ground plane, and C_f is the fringing capacitance due to edge conductor [6]:

$$C_f = \frac{1}{2}\left[\frac{\sqrt{\varepsilon_{\text{eff}}}}{cZ_c - C_p}\right], \tag{1}$$

where $c = 3\times10^8$ m/s and Z_c are the characteristic impedance of the line and ε_{eff} is the effective dielectric constant of substrate [7]. Since there is another line due to the presence

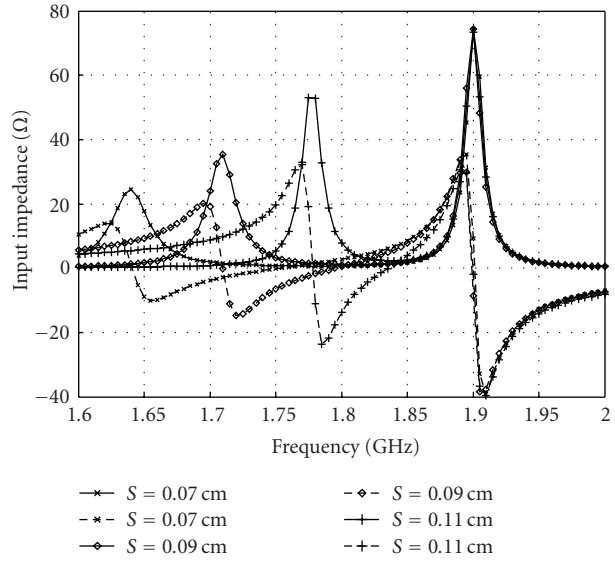

Figure 4: Variation of input impedance with frequency for different gap length at C = 3.001 cm.

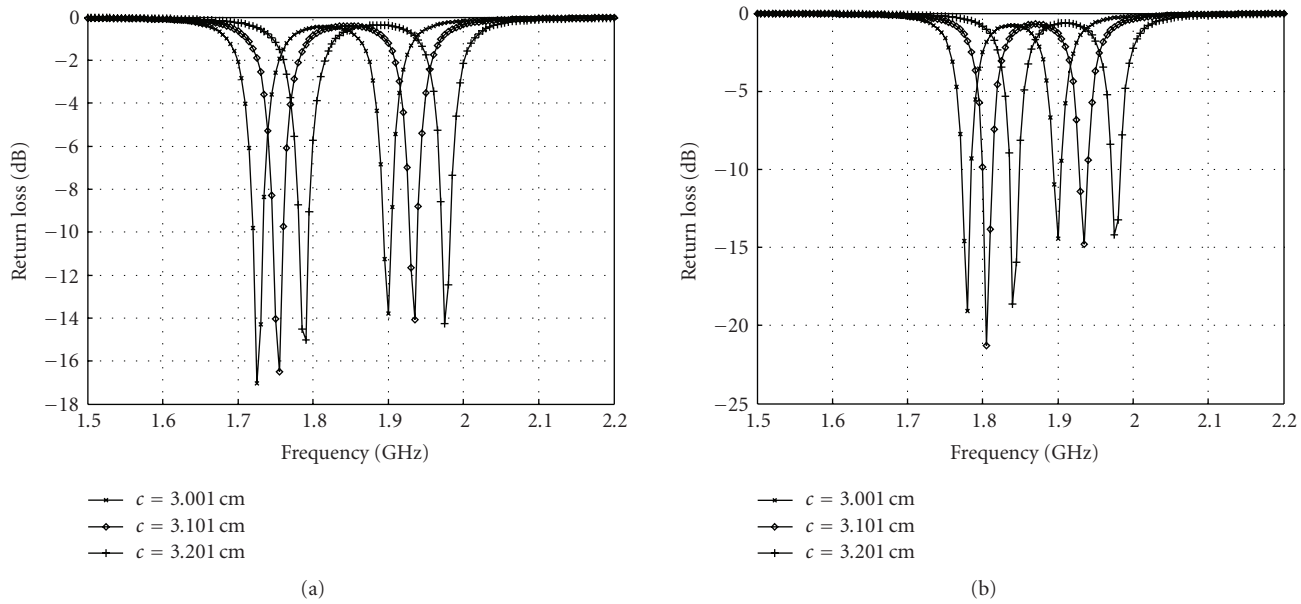

FIGURE 5: (a) Variation of return loss with frequency for different feed location at $S = 0.095$ cm. (b) Variation of return loss with frequency for different feed location at $S = 0.11$ cm.

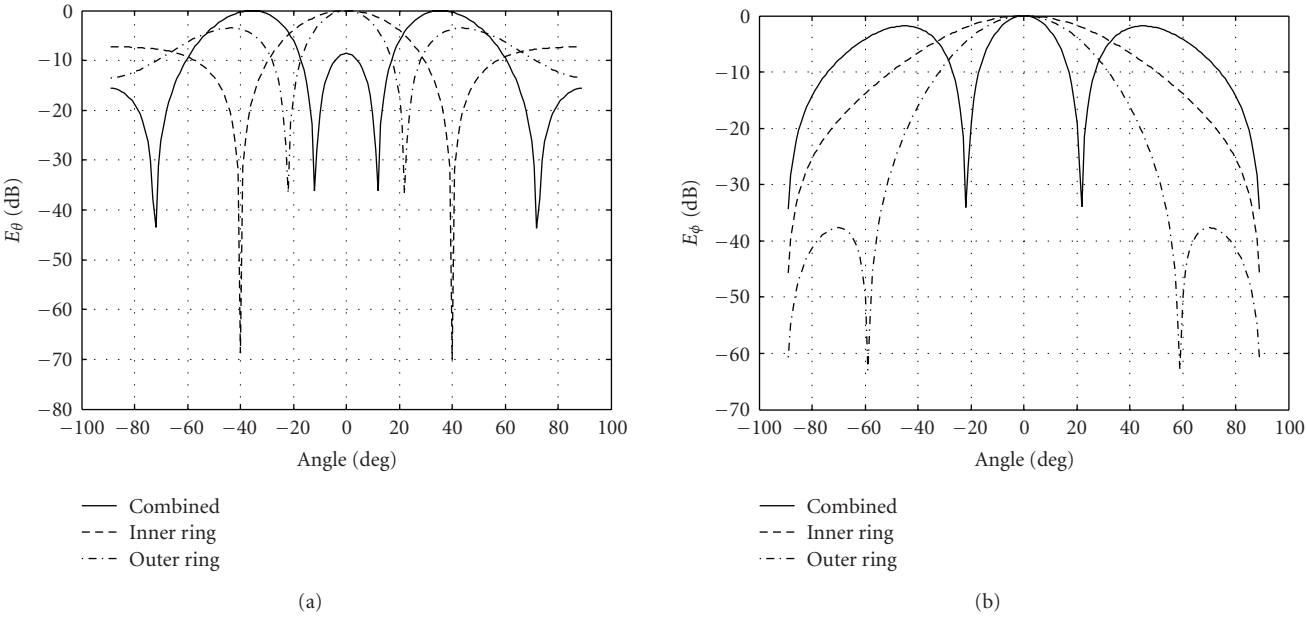

FIGURE 6: (a) Variation of radiation pattern E_θ with angle for $S = 0.095$ cm. (b) Variation of radiation pattern E_ϕ with angle for $S = 0.095$ cm.

of parasitic element, there is some modification in fringe capacitance as [6]

$$C'_f = C_f\left[1 + A\left(\frac{h}{s}\right)\tanh\left(\frac{10s}{h}\right)\right]^{-1}\left(\frac{\varepsilon_r}{\varepsilon_{\text{eff}}}\right)^{1/2}, \qquad (2)$$

where $A = \exp(-0.1\exp(2.33 - 2.53\,w/h))$.

The odd mode capacitance is as shown in Figure 2(a) and given by $C_{\text{odd}} = C_p + C_f + C_{\text{gd}} + C_{\text{ga}}$, where C_{gd} is the capacitance between two strip lines through dielectric region, and C_{ga} is the capacitance between two strip lines through air.

The gap capacitance

$$C_{\text{ga}} = \frac{1}{2}K(k')\frac{\varepsilon_0}{K(k)}, \qquad (3)$$

where $K(k)$ and $K(k')$ are elliptic functions. Reference [5] defined as

$$k = \frac{s/h}{(s/h) + 2(w/h)}, \qquad k' = \sqrt{1 - k^2},$$

Table 1: Designing specification of annular ring microstrip antenna.

Parameters	Value
Substrate material used	RT Duroid 5870
Effective relative permittivity	$\varepsilon_{\text{eff}} = 2.1936$
Relative permittivity of the substrate	$\varepsilon_r = 2.32$
Thickness of dielectric substrate	$h = 0.159$ cm
Inner radius of the inner ring	$a_1 = 3$ cm
Outer radius of the inner ring	$b_1 = 6$ cm
Feed point of the inner ring	$c = 3.35$ cm
Inner radius of outer ring	$a_2 = 6.05$ cm.
Outer radius of outer ring	$b_2 = 9.05$ cm.

$$\frac{K(k')}{K(k)} = \begin{cases} \dfrac{1}{\pi}\ln\left[2\dfrac{1+\sqrt{k'}}{1-\sqrt{k'}}\right], & 0 \le k \le 0.5, \\ \dfrac{\pi}{\ln\left[2\left(\left(1+\sqrt{k}\right)/\left(1-\sqrt{k}\right)\right)\right]}, & 0 \le k \le 1. \end{cases} \tag{4}$$

Since the two strips have the electric flux between the air dielectric region so capacitance

$$C_{\text{gd}} = \left(\frac{\varepsilon_0\varepsilon_r}{\pi}\right)\ln\left\{\cot h\frac{\pi s}{4h}\right\} + 0.65C_f\left[\frac{0.02}{(s/h)}\sqrt{\varepsilon_r} + 1 - \frac{1}{\varepsilon_r^2}\right]. \tag{5}$$

2.2. ARMSA analysis

The gap-coupled ARMSA can be represented as the two parallel microstrip lines. The equivalent circuit for ARMSA can be expressed as the parallel combination of Y_1, L_1, C_1 and Y_2, L_2, C_2, where the subscript 1 represents for inner ring and 2 for the outer parasitic ring. The value of Y_1, L_1, C_1 can be written as [8]

$$L_1 = \frac{\mu h}{\pi k_1^2[n,m]}\left[J_n(k_1c)\,Y_n'(k_1a_e) - Y_n(k_1c)J_n'(k_1a_e)\right]^2, \tag{6}$$

where

$$[n,m] = \frac{1}{2k_1^2}\left[(k_1^2b_1^2-1)\left\{J_n(k_1b_{1e})\,Y_n'(k_1a_{1e}) - Y_n'(k_1b_{1e})J_n'(k_1a_{1e})\right\}^2 - \frac{4}{\pi^2k_1^2a_{1e}}(k_1^2a_{1e}^2-1)\right],$$

$$C_1 = \frac{\mu\varepsilon_0\varepsilon_r}{L_1k_1^2},$$

$$Y_1 = \frac{\pi}{h}\left[\left(\frac{E_a}{E_b}\right)^2 g(a,a) + \left(\frac{E_b}{E_c}\right)^2 g(b,b) - 2\frac{E_aE_b}{E_c^2}y(a,b)\right]. \tag{7}$$

The values of L_2, C_2, and Y_2 are obtained for the outer parasitic ring using (6), (7) for the inner ring of the antenna. The equivalent circuit for gap-coupled ARMSA can be given as in Figures 3(a) and 3(b) for even and odd mode cases.

2.3. Impedance of gap-coupled ARMSA

Due to the presence of the parasitic ARMSA, the input impedance of gap-coupled ARMSA differs from the impedance of single ARMSA. The effective dielectric constant is due to the fringing and various other factors which can be calculated for even mode $\varepsilon_{\text{re}}^e$ and odd mode $\varepsilon_{\text{re}}^0$ using even and odd mode capacitances [8] as

$$\varepsilon_{\text{re}}^e = \frac{C_e}{C_e^a}, \qquad \varepsilon_{\text{re}}^0 = \frac{C_0}{C_0^a}, \tag{8}$$

where C_e^a and C_0^a are the even and odd mode capacitances for the gap-coupled ARMSA with air as dielectric. With the help of these dielectric constants and the equivalent circuit model (Figures 3(a) and 3(b)), input impedance for even mode, $Z_{\text{in}}(e)$, and for odd mode, $Z_{\text{in}}(0)$, are calculated separately by putting even and odd mode relative permittivity (given in (8)), respectively. The input impedance of gap-coupled ARMSA is now written as [6] $Z_{\text{in}} = Z_{\text{in}}(e) + Z_{\text{in}}(0)$.

The return loss can be calculated as

$$R = 20\,\log\left(|\Gamma|\right). \tag{9}$$

2.4. Radiation patterns

The radiation pattern of the ARMSA is due to the superposition of the fields radiated by all the apertures. The radiation patterns of the N apertures are [9]

$$E_\theta = \left[\sum_{m=1}^{N} a_mE_{am}J_1'(k_0a_m\sin\theta) - \sum_{m=1}^{N} b_mE_{bm}J_1'(k_0b_m\sin\theta)\right]\cos\phi,$$

$$E_\phi = \left[\sum_{m=1}^{N} E_{am}J_1(k_0a_m\sin\theta) - \sum_{m=1}^{N} E_{bm}J_1(k_0b_m\sin\theta)\right]\cot\theta\sin\phi, \tag{12a}$$

where E_{am} and E_{bm} are the electric field at the inner and outer peripheries of the mth ring, respectively. We are considering only two rings, therefore, the radiation pattern of the ARMSA is obtained by putting $m = 1$ and 2 in the above equations.

3. DESIGN PARAMETERS

The gap-coupled ARMSA is designed with the following specifications as given in Table 1.

4. DISCUSSION OF RESULTS

Figure 4 shows the variation of input impedance with frequency for different gap length for particular feed location of 3.001 cm. It is observed that the lower band shows the different resonant frequencies of 1.727 GHz and 1.778 GHz for different gap lengths of 0.095 cm. and 0.11 cm, however, for an upper band of gap-coupled ARMSA, the resonance frequency is approximately the same for different gap length.

Table 2: Peak value of input impedance, resonance frequency for upper and lower band for different feed locations.

Gap length →	S = 0.095 cm				S = 0.100 cm				S = 0.110 cm			
Feed point ↓	P_{lower}* (ohms)	P_{upper}** (ohms)	F_{lower}# (GHz)	F_{upper}## (GHz)	P_{lower} (ohms)	P_{upper} (ohms)	F_{lower} (GHz)	F_{upper} (GHz)	P_{lower} (ohms)	P_{upper} (ohms)	F_{lower} (GHz)	F_{upper} (GHz)
c = 3.001 cm	39.40	74.08	1.727	1.899	43.58	73.93	1.744	1.899	53.05	73.30	1.778	1.900
c = 3.101 cm	37.55	72.15	1.754	1.934	43.62	72.06	1.771	1.934	55.90	71.75	1.806	1.934
c = 3.201 cm	36.50	65.02	1.788	1.977	42.35	64.16	1.806	1.977	53.20	65.50	1.842	1.977

* P_{lower}: The peak value of input impedance for lower band.
** P_{upper}: The peak value of input impedance for lower band.
# F_{lower}: The resonance frequency for lower band.
F_{upper}: The resonance frequency for upper band.

Table 3: Peak value of input impedance, resonance frequency for upper and lower band for different gap lengths.

Feed point →	c = 3.001 cm				c = 3.101 cm				c = 3.201 cm			
Gap length ↓	P_{lower} (ohms)	P_{upper} (ohms)	F_{lower} (GHz)	F_{upper} (GHz)	P_{lower} (ohms)	P_{upper} (ohms)	F_{lower} (GHz)	F_{upper} (GHz)	P_{lower} (ohms)	P_{upper} (ohms)	F_{lower} (GHz)	F_{upper} (GHz)
S = 0.09 cm	35.39	74.31	1.710	1.899	34.81	72.41	1.736	1.9337	33.61	65.33	1.770	1.9771
S = 0.10 cm	43.58	73.93	1.744	1.899	43.62	72.06	1.771	1.9338	42.35	64.16	1.806	1.9771
S = 0.11 cm	53.05	73.30	1.778	1.900	55.90	71.74	1.806	1.9343	53.20	65.49	1.842	1.9774

This type of characteristic can be used for different applications. It is also observed that peak value of real part of the input impedance for lower patch increases with increasing gap length. The variation of input impedance with frequency for different feed location and gap length is also verified from Tables 2 and 3, respectively.

The return loss of gap-coupled ARMSA is shown in Figures 5(a)-5(b) for different value of gap length and feed locations. Return loss of lower band decreases with increasing the feed point, while it decreases with increasing the feed point for upper band. It is also observed that the bandwidth of lower band decreases with increasing the feed point, however, the bandwidth of upper band increases with increasing the feed point for a different gap length.

The radiation pattern of the gap-coupled annular ring microstrip antenna in the direction of elevation and azimuth plane is shown in Figures 6(a)-6(b), respectively. It is observed that the beamwidth of gap-coupled annular patch is lower than the individual annular patch but the side lobes of gap-coupled annular patch are higher than the individual annular ring patch because enhancement in radiation power due to parasitic element is not accompanied by an increase in ohmic loss of the system.

5. CONCLUSION

The new technique to gap-coupled with parasitic element shows the tunability in frequency and also dual band operation. Efficiency of an antenna can be used where large bandwidth and tunable frequency is required.

REFERENCES

[1] W. Chew, "A broad-band annular-ring microstrip antenna," *IEEE Transactions on Antennas and Propagation*, vol. 30, no. 5, pp. 918–922, 1982.

[2] B. K. Kanaujia and B. R. Vishvakarma, "Some investigations on annular ring microstrip antenna," in *Proceedings of the IEEE Antennas and Propagation Society International Symposium*, vol. 3, pp. 466–469, San Antonio, Tex, USA, June 2002.

[3] G. Kompa and R. Mehran, "Planar waveguide model for calculating microstrip components," *Electronics Letters*, vol. 11, no. 19, pp. 459–460, 1975.

[4] A. K. Bhattacharyya and R. Garg, "Input impedance of annular ring microstrip antenna using circuit theory approach," *IEEE Transactions on Antennas and Propagation*, vol. 33, no. 4, pp. 369–374, 1985.

[5] R. Garg, "Design equations for coupled microstrip lines," *International Journal of Electronics*, vol. 47, no. 6, pp. 587–591, 1979.

[6] C. K. Aanandan, P. Mohanan, and K. G. Nair, "Broad-band gap coupled microstrip antenna," *IEEE Transactions on Antennas and Propagation*, vol. 38, no. 10, pp. 1581–1586, 1990.

[7] W. F. Richards, Y. T. Lo, and D. D. Harrison, "An improved theory for microstrip antennas and applications," *IEEE Transactions on Antennas and Propagation*, vol. 29, no. 1, pp. 38–46, 1981.

[8] B. K. Kanaujia and B. R. Vishvakarma, "Analysis of two-concentric annular ring microstrip antenna," *Microwave and Optical Technology Letters*, vol. 36, no. 2, pp. 104–108, 2003.

[9] A. K. Bhattacharyya and R. Garg, "A microstrip array of concentric annular rings," *IEEE Transactions on Antennas and Propagation*, vol. 33, no. 6, pp. 655–659, 1985.